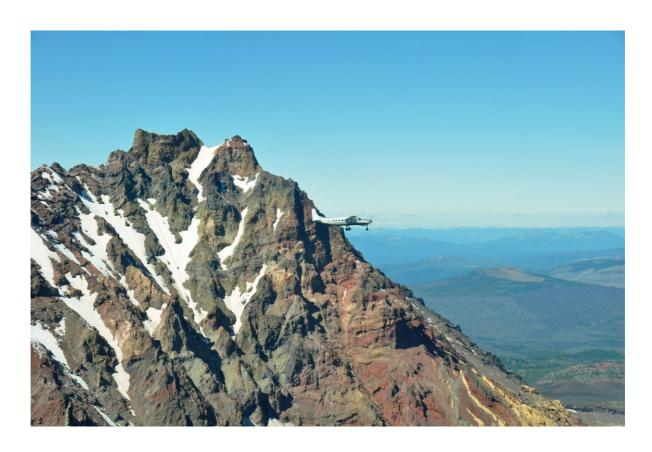


LIDAR REMOTE SENSING DATA COLLECTION:

DOGAMI, DESCHUTES STUDY AREA

TABLE OF CONTENTS

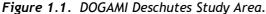
| 1. Overview | 1 |
|--|----|
| 1.1 Study Area | 1 |
| 1.2 Delivery Areas | 2 |
| 1.3 Area 16 Boundary | |
| 2. Acquisition | |
| 2.1 Airborne Survey Overview - Instrumentation and Methods | 6 |
| 2.2 Ground Survey - Instrumentation and Methods | |
| 2.2.1 Instrumentation | |
| 2.2.2 Monumentation | 8 |
| 2.2.3 Methodology | 13 |
| 3. Accuracy | |
| 3.1 Relative Accuracy | |
| 3.2 Absolute Accuracy | |
| 4. Data Density/Resolution | |
| 5. Certifications | |
| 6. Selected Imagery | 39 |

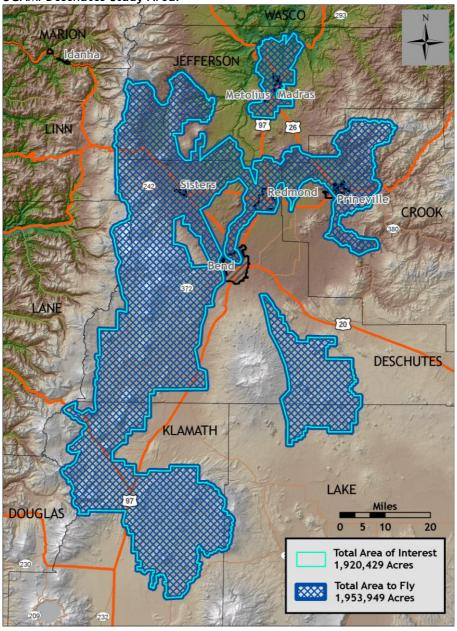


1. Overview

1.1 Study Area

Watershed Sciences, Inc. has collected Light Detection and Ranging (LiDAR) data of the Deschutes Study Area for the Oregon Department of Geology and Mineral Industries (DOGAMI). The area of interest (AOI) totals 3,001 square miles (1,920,429 acres) and the total area flown (TAF) covers 3,053 square miles (1,953,949 acres). The TAF acreage is greater than the original AOI acreage due to buffering and flight planning optimization (**Figure 1.1** below). DOGAMI data are delivered in OGIC (HARN): Projection: Oregon Statewide Lambert Conformal Conic; horizontal and vertical datum: NAD83 (HARN)/NAVD88 (Geoid03); units: International Feet.

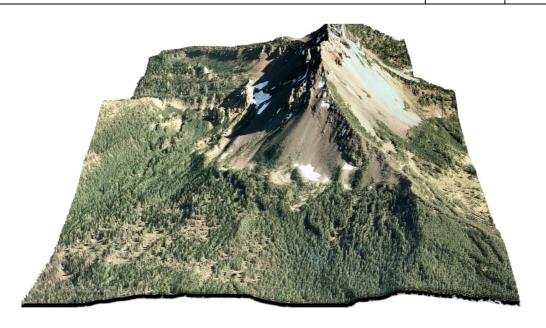


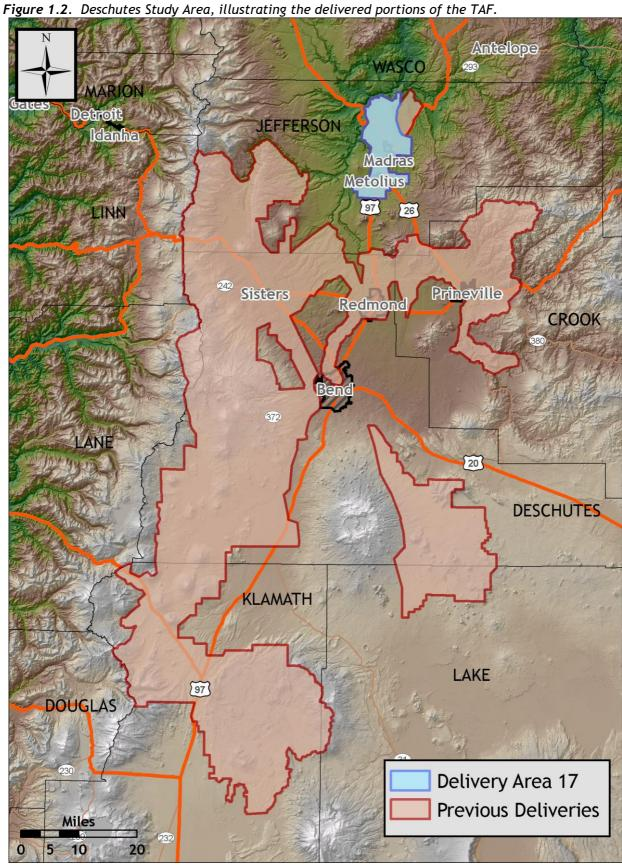


1.2 Delivery Areas

Acreage per delivery is detailed below and in Figure 1.2.

| DOGAMI Deschutes Study Area | | | | | |
|-----------------------------|--------------------|--|-----------|-----------|--|
| | Delivery Date | Acquisition Dates | AOI Acres | TAF Acres | |
| Delivery Area 1 | January 5, 2010 | Oct. 2, 2009 | 12,731 | 13,507 | |
| Delivery Area 2 | February 26, 2010 | Oct. 5 - 11, 2009 | 76,828 | 78,268 | |
| Delivery Area 3 | March 5, 2010 | Oct. 11-17, 2009 | 111,073 | 113,101 | |
| Delivery Area 4 | April 9, 2010 | Oct. 7 - 11, 2009 | 163,164 | 163,814 | |
| Delivery Area 5 | March 5, 2010 | Oct. 1-12, 2009 | 78,577 | 80,720 | |
| Delivery Area 6 | March 12, 2010 | Oct. 17-23, 2009 | 54,681 | 55,470 | |
| Delivery Area 7 | March 23, 2010 | Oct. 18-20; Nov 1-4 2009 | 150,214 | 151,426 | |
| Delivery Area 8 | April 16, 2010 | Oct. 8-23, 2009 | 100,314 | 102,343 | |
| Delivery Area 9 | September 3, 2010 | Oct. 11-16, 2009; June 14, 2010 | 30,161 | 31,969 | |
| Delivery Area 10 | September 3, 2010 | Oct. 12-17, 2009 May 29-June 17, 2010 | 48,746 | 50,833 | |
| Delivery Area 11 | September 22, 2010 | Oct. 16-Nov 5, 2009 May 28 - July 3, 2010 | 229,197 | 231,807 | |
| Delivery Area 12 | October 29, 2010 | Oct. 16-Nov 5, 2009 May 28 - July 3, 2010 | 169,905 | 172,978 | |
| Delivery Area 13 | January 14, 2010 | Aug. 25 - Sept. 6, 2010 | 319,866 | 324,153 | |
| Delivery Area 14 | January 14, 2010 | Sept. 5-11, 2010 | 32,354 | 33,500 | |
| Delivery Area 15 | January 14, 2010 | Sept 6-13, 2010 | 205,833 | 210,184 | |
| Delivery Area 16 | January 14, 2010 | Sept 10-12, 2010 | 73,097 | 74,086 | |
| Delivery Area 17 | May 25, 2011 | Nov 17-19, 2010; Mar 10-11, 2011; May 5, 2011 | 63,688 | 65,790 | |
| | 1,920,429 | 1,953,949 | | | |





1.3 Area 16 Boundary

Owing to differences in snow and ice surfaces and erosion/deposition topography related to time period differences in data acquisition for Deschutes Area 16, there is a "hard line" between data acquired in 2009 and 2010. The data cannot be overlapped between years due to an abundance of features exhibiting temporal change over the 1-year span in acquisition time. The dataset remains seamless across permanent surfaces such as roads, and will only show differences along the "hard line" describing the acquisition boundary for each year (see images below). This seam is provided in shapefile format.

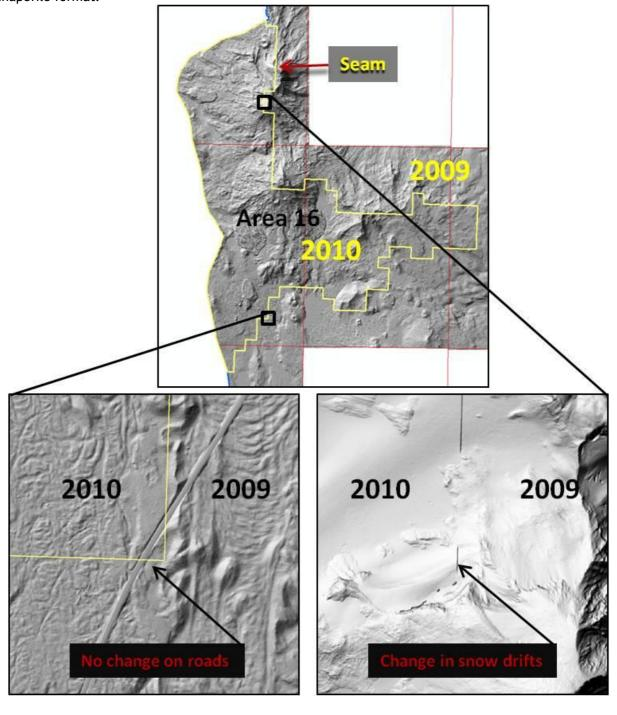


Figure 1.3. Deschutes Study Area, illustrating the delivered 7.5 minute USGS quads. 412262 4412261 4412168 4412167 4412166 4412165 4412164 4412163 4412162 4412161 4412068 4412067 4412066 44120 44122F2 44122F1 44121F8 44121F7 44121F6 44121F5 44121F4 44121F3 44121F2 44121F1 44120F8 44120F7 44120F6 44120F5 44122E2 44122E1 44121E8 44121E7 44121E6 44121E5 44121E4 44121E3 44121E2 44121E1 44120E8 44120E7 44120E6 44120E5 44122D2 44122D1 44121D8 44121D7 44121D6 44121D5 44121D4 44121D3 44121D2 44121D1 44120D8 44120D7 44120D6 44120D5 44122C2 44122C1 44121C8 44121C7 44121C6 44121C5 44121C4 44121C3 44121C2 44121C1 44120C8 44120C7 44120C6 44120C5 4412282 4412281 4412188 4412187 4412186 4412185 4412184 4412183 4412182 4412181 4412088 4412087 4412086 4412085 44122A2 44122A1 44121A8 44121A7 44121A6 44121A5 44121A4 44121A3 44121A2 44121A1 44120A8 44120A7 44120A6 44120A5 43122H2 43122H1 43121H8 43121H7 43121H6 43121H5 43121H4 43121H3 43121H2 43121H1 43120H8 43120H7 43120H6 43120H6 4312262 4312261 4312168 4312167 4312166 4312165 4312164 4312163 4312162 4312161 4312068 4312067 4312066 4312065 43122F2 43122F1 43121F8 43121F7 43121F6 43121F5 43121F4 43121F3 43121F2 43121F1 43120F8 43120F7 43120F6 43120F5 43122E2 43122E1 43121E8 43121E7 43121E6 43121E5 43121E4 43121E3 43121E2 43121E1 43120E8 43120E7 43120E6 43120E5 43122D2 43122D1 43121D8 43121D7 43121D6 43121D5 43121D4 43121D3 43121D2 43121D1 43120D8 43120D7 43120D6 43120D5 43122C2 43122C1 43121C8 43121C7 43121C6 43121C5 43121C4 43121C3 43121C2 43121C1 43120C8 43120C7 43120C6 43120C5

4312282 4312281 4312188 4312187 4312186 4312185 4312184 4312183 4312182 4312181 4312088 4312087 4312086 4312085

43122A2 43122A1 43121A8 43121A7 43121A6 43121A5 43121A4 43121A3

Data Delivery Complete

7.5-Min USGS Quad

2. Acquisition

2.1 Airborne Survey Overview - Instrumentation and Methods

The LiDAR survey utilized Leica ALS50 Phase II and ALS60 sensors mounted in multiple Cessna Caravan 208Bs. The Leica systems were set to acquire $\geq 105,000$ laser pulses per second (i.e. 105 kHz pulse rate) and flown at 900 and 1300 meters above ground level (AGL), capturing a scan angle of $\pm 14^{\circ}$ from nadir¹. These settings are developed to yield points with an average native density of ≥ 8 points per square meter over terrestrial surfaces. The native pulse density is the number of pulses emitted by the LiDAR system. Some types of surfaces (i.e. dense vegetation or water) may return fewer pulses than the laser originally emitted. Therefore, the delivered density can be less than the native density and vary according to distributions of terrain, land cover and water bodies.



The Cessna Caravan is a powerful, stable platform, which is ideal for the often remote and mountainous terrain found in the Pacific Northwest. The Leica ALS60 sensor head installed in the Caravan is shown on the right.

Table 2.1 LiDAR Survey Specifications

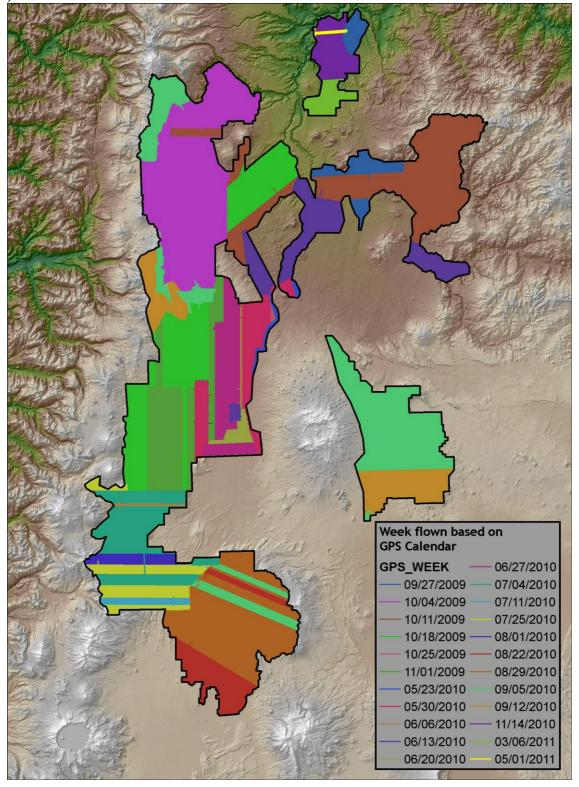
| Sensors | Leica ALS50 Phase II and ALS60 |
|------------------------|--------------------------------|
| Survey Altitudes (AGL) | 900 m and 1300 m |
| Pulse Rate | >105 kHz |
| Pulse Mode | Single |
| Mirror Scan Rate | 52 Hz |
| Field of View | 28° (±14° from nadir) |
| Roll Compensated | Up to 15° |
| Overlap | 100% (50% Side-lap) |

The study area was surveyed with opposing flight line side-lap of $\geq 50\%$ ($\geq 100\%$ overlap) to reduce laser shadowing and increase surface laser painting. The system allows up to four range measurements per pulse, and all discernable laser returns were processed for the output dataset.

To solve for laser point position, it is vital to have an accurate description of aircraft position and attitude. Aircraft position is described as x, y and z and measured twice per second (2 Hz) by an onboard differential GPS unit. Aircraft attitude is measured 200 times per second (200 Hz) as pitch, roll and yaw (heading) from an onboard inertial measurement unit (IMU). **Figure 2.1** shows the flight lines completed for the study area.

¹ Nadir refers to the perpendicular vector to the ground directly below the aircraft. Nadir is commonly used to measure the angle from the vector and is referred to a "degrees from nadir".

Figure 2.1. Actual flightlines for the Deschutes Study Area illustrating the dates flown (based on GPS week).



2.2 Ground Survey - Instrumentation and Methods

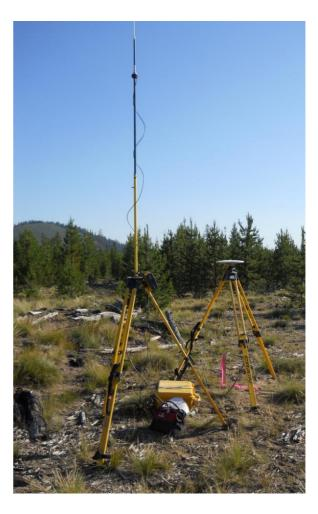
During the LiDAR survey, static (1 Hz recording frequency) ground surveys were conducted over either known or set monuments. Monument coordinates are provided in **Table 2.2** and shown in **Figure 2.2** for the AOI. After the airborne survey, the static GPS data were processed using triangulation with continuous operation stations (CORS) and checked using the Online Positioning User Service (OPUS²) to quantify daily variance. Multiple sessions were processed over the same monument to confirm antenna height measurements and reported position accuracy.

2.2.1 Instrumentation

The Global Navigation Satellite System (GNSS³) survey utilized a Trimble GPS receiver model R7 with a Zephyr Geodetic antenna and ground plane for static control points. A Trimble GPS R8 unit was primarily used for gathering Real Time Kinematic (RTK) locations but was also used as a static receiver when necessary. For RTK data, the collector began recording after remaining stationary for 5 seconds then calculated the pseudo range position from at least three epochs with the relative error under 1.5cm horizontal and 2cm vertical. All GPS measurements were made with dual frequency L1-L2 receivers with carrier-phase correction.

2.2.2 Monumentation

Whenever possible, existing and established survey benchmarks served as control points during LiDAR acquisition, including those previously set by Watershed Sciences. In addition to the National Geodetic Survey (NGS) monuments, the county surveyor's offices and Oregon Department of Transportation (ODOT) often establish their own benchmarks. NGS benchmarks are preferred for control points. Watershed Sciences produced our own monuments in the absence of NGS benchmarks, county surveys, or ODOT monumentation. These monuments were spaced at a minimum of one mile and every effort was made to keep these monuments within the public right of way. If monuments were required on private property, consent from the owner was obtained. All monumentation was done with 5/8" x 24" or 30" rebar topped with an orange plastic cap (prior to January, 2010) and with an aluminum cap (from January 2010 to present).



² Online Positioning User Service (OPUS) is run by the National Geodetic Survey to process corrected monument positions.

³ GNSS: Global Navigation Satellite System consisting of the U.S. GPS constellation and Soviet GLONASS constellation

Figure 2.2. Base stations for the Deschutes Study Area.

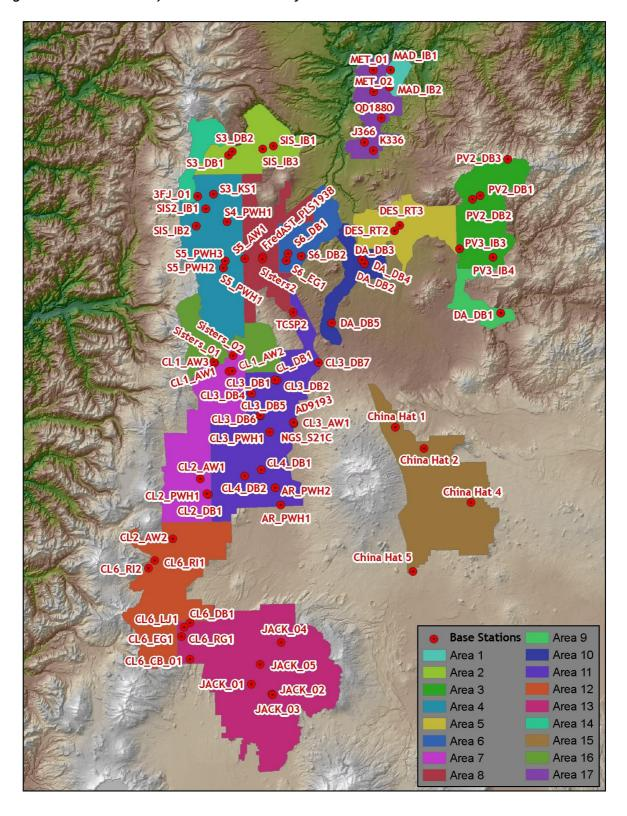


Table 2.2. Base Station Surveyed Coordinates, (NAD83/NAVD88, OPUS corrected) used for kinematic post-processing of the aircraft GPS data for the Deschutes Study Area in **2009**.

| cessing of the uneraj | Datum NAD83 (HARN) | | GRS80 |
|-----------------------|--------------------|------------------|----------------------|
| Base Stations ID | Latitude (North) | Longitude (West) | Ellipsoid Height (m) |
| CL1_AW1 | 44 00 11.68842 | 121 40 50.12824 | 1914.182 |
| CL1_AW2 | 44 00 16.69262 | 121 40 04.34254 | 1899.735 |
| CL1_AW3 | 44 01 31.45566 | 121 43 48.33634 | 1637.650 |
| CL2_AW1 | 43 44 01.10212 | 121 47 08.62177 | 1298.569 |
| CL2_AW2 | 43 35 1.53931 | 121 53 3.72446 | 1334.811 |
| CL2_DB1 | 43 41 36.78416 | 121 45 29.96714 | 1300.030 |
| CL2_PWH1 | 43 41 47.61505 | 121 45 49.78708 | 1300.985 |
| CL3_DB1 | 43 58 48.63125 | 121 31 14.42329 | 1602.125 |
| DES_RT2 | 44 20 56.78639 | 121 05 28.44007 | 847.267 |
| DES_RT3 | 44 21 48.46263 | 121 04 21.28445 | 839.760 |
| FredAST_PLS1938 | 44 17 25.33409 | 121 33 18.25920 | 953.378 |
| MAD_IB1 | 44 45 17.99134 | 121 05 30.55012 | 638.251 |
| MAD_IB2 | 44 42 43.10030 | 121 05 50.80549 | 641.072 |
| PV2_DB1 | 44 25 57.61697 | 120 47 13.34425 | 986.631 |
| PV2_DB2 | 44 25 24.97372 | 120 48 51.76166 | 967.022 |
| PV2_DB3 | 44 31 21.94274 | 120 41 10.80400 | 1537.742 |
| PV3_IB3 | 44 18 00.14713 | 120 51 50.79538 | 953.144 |
| S3_DB1 | 44 32 53.93542 | 121 40 09.12051 | 948.395 |
| S3_DB2 | 44 33 28.00859 | 121 39 20.60152 | 937.014 |
| S3_KS1 | 44 27 02.22135 | 121 43 29.33220 | 990.974 |
| S4_PWH1 | 44 22 52.59100 | 121 40 41.21292 | 1005.952 |
| S5_AW1 | 44 17 11.13065 | 121 37 05.09836 | 1009.735 |
| S5_PWH1 | 44 15 50.54444 | 121 41 36.40461 | 1277.950 |
| S5_PWH2 | 44 15 52.54934 | 121 41 36.18206 | 1274.839 |
| S5_PWH3 | 44 16 55.30769 | 121 41 11.96243 | 1184.015 |
| S6_DB1 | 44 17 50.87280 | 121 27 57.61082 | 923.456 |
| S6_DB2 | 44 17 26.98022 | 121 25 12.17361 | 909.928 |
| S6_EG1 | 44 16 48.49596 | 121 28 22.62132 | 928.845 |
| SIS_IB1 | 44 34 09.04366 | 121 30 37.46176 | 1083.141 |
| SIS_IB2 | 44 22 17.16094 | 121 47 11.84116 | 1512.582 |
| SIS_IB3 | 44 33 46.29685 | 121 32 56.15898 | 1179.887 |
| SIS2_IB1 | 44 24 49.84091 | 121 45 07.82346 | 1081.530 |
| Sisters2 | 44 17 6.32589 | 121 33 21.56444 | 957.216 |

Table 2.2 continued. Base Station Surveyed Coordinates for **2010**.

| | Datum NAD83 (HARN) | | GRS80 |
|------------------|--------------------|------------------|----------------------|
| Base Stations ID | Latitude (North) | Longitude (West) | Ellipsoid Height (m) |
| 3FJ_01 | 44 26 44.81912 | 121 46 46.17402 | 1292.511 |
| AD9193 | 43 52 10.29925 | 121 27 22.07928 | 1247.736 |
| AR_PWH1 | 43 39 50.63378 | 121 30 27.01222 | 1267.949 |
| AR_PWH2 | 43 42 30.82766 | 121 31 33.70042 | 1272.459 |
| China Hat 1 | 43 51 16.53733 | 121 06 12.45141 | 1409.420 |
| China Hat 2 | 43 47 57.53358 | 121 00 21.46747 | 1401.952 |
| China Hat 4 | 43 39 36.37642 | 120 50 50.34971 | 1530.983 |
| China Hat 5 | 43 29 23.42275 | 121 03 15.98832 | 1354.250 |
| CL_DB1 | 43 58 48.63113 | 121 31 14.42360 | 1602.116 |
| CL3_AW1 | 43 52 18.84340 | 121 27 26.18486 | 1246.968 |
| CL3_DB2 | 43 58 45.87969 | 121 30 46.67609 | 1592.403 |
| CL3_DB4 | 43 56 49.54149 | 121 36 05.95067 | 1595.515 |
| CL3_DB5 | 43 53 26.35760 | 121 34 23.85087 | 1328.108 |
| CL3_DB6 | 43 53 26.22688 | 121 34 23.36053 | 1328.016 |
| CL3_DB7 | 44 01 17.70630 | 121 22 01.03065 | 1160.175 |
| CL3_PWH1 | 43 50 57.47490 | 121 32 27.64700 | 1308.667 |
| CL4_DB1 | 43 45 16.21200 | 121 34 24.59759 | 1277.331 |
| CL4_DB2 | 43 44 21.63368 | 121 37 51.06188 | 1291.539 |
| CL6_CB_01 | 43 16 46.83888 | 121 49 48.26069 | 1532.563 |
| CL6_DB1 | 43 22 16.05575 | 121 49 43.73159 | 1427.186 |
| CL6_EG1 | 43 20 14.66889 | 121 51 27.23403 | 1456.314 |
| CL6_LJ1 | 43 21 36.87373 | 121 50 53.89536 | 1458.876 |
| CL6_RG1 | 43 20 14.66851 | 121 51 27.23345 | 1456.325 |
| CL6_RI1 | 43 31 45.45490 | 121 56 50.29620 | 1433.901 |
| CL6_RI2 | 43 30 37.29478 | 121 58 11.09399 | 1435.572 |
| DA_DB1 | 44 8 7.40991 | 120 43 36.67908 | 1053.103 |
| DA_DB2 | 44 16 06.78328 | 121 11 58.23563 | 898.107 |
| DA_DB3 | 44 16 42.37582 | 121 12 25.86302 | 885.921 |
| DA_DB4 | 44 16 42.38773 | 121 12 26.37018 | 885.848 |
| DA_DB5 | 44 7 14.92788 | 121 19 3.65407 | 1023.762 |
| J366 | 44 34 28.09220 | 121 11 23.51740 | 755.906 |
| JACK_01 | 43 12 50.23290 | 121 37 10.90309 | 1576.463 |
| JACK_02 | 43 11 19.54846 | 121 32 57.93613 | 1512.609 |
| JACK_03 | 43 11 12.54826 | 121 32 50.01047 | 1513.491 |
| JACK_04 | 43 19 07.80212 | 121 30 52.54466 | 1643.444 |
| JACK_05 | 43 15 49.33136 | 121 35 18.61995 | 1619.393 |
| K336 | 44 33 10.66948 | 121 9 34.38785 | 774.577 |
| NGS_S21C | 43 52 10.42129 | 121 27 21.97904 | 1247.666 |
| PV3_IB4 | 44 16 36.11242 | 120 44 53.73911 | 1072.697 |
| QD1880 | 44 38 02.20664 | 121 7 40.23749 | 663.297 |
| Sisters_01 | 44 01 41.78953 | 121 43 54.67823 | 1635.938 |

Table 2.2 continued. Base Station Surveyed Coordinates for 2010 (continued from previous page).

| Sisters_02 | 44 02 34.47069 | 121 39 53.94907 | 2046.817 |
|------------|----------------|-----------------|----------|
| TCSP2 | 44 8 59.52851 | 121 27 5.94067 | 1050.741 |

Table 2.2 continued. Base Station Surveyed Coordinates for 2011.

| | Datum NAD83 (HARN) | | GRS80 |
|------------------|-----------------------------------|----------------|----------------------|
| Base Stations ID | Latitude (North) Longitude (West) | | Ellipsoid Height (m) |
| MET_01 | 44 45 20.52235 | 121 9 11.57529 | 693.006 |
| MET_02 | 44 42 3.38964 | 121 9 12.21175 | 714.230 |

2.2.3 Methodology

Each aircraft was assigned a ground crew member with two R7 receivers and an R8 receiver. The ground crew vehicles were equiped with standard field survey supplies and equipment including safety materials. All data points were observed for a minimum of two survey sessions lasting no fewer than 6 hours. At the beginning of every session the tripod and antenna were reset, resulting in two independent instrument heights and data files. Data were collected at a rate of 1Hz using a 10 degree mask on the antenna.

The ground crew uploaded the GPS data to the FTP site on a daily basis to be returned to the office for PLS oversight, QA/QC review and processing. OPUS processing triangulated the monument position using 3 CORS stations resulting in a fully adjusted position. CORPSCON⁴ 6.0.1 software was used to convert the geodetic positions from the OPUS reports. After multiple days of data had been collected at each monument, accuracy and error ellipses were calculated. This information allowed for the rating of each monument based on FGDC-STD-007.2-1998⁵ Part 2 table 2.1 at the 95% confidence level.

All GPS measurements were made during periods with PDOP less than or equal to 3.0 and with at least 6 satellites in view of both a stationary reference receiver and the roving receiver. RTK positions were collected on 20% of the flight lines and on bare earth locations such as paved, gravel or stable dirt roads, and other locations where the ground was clearly visible (and was likely to remain visible) from the sky during the data acquisition and RTK measurement period(s). In order to facilitate comparisons with LiDAR measurements, RTK measurements were not taken on highly reflective surfaces such as center line stripes or lane markings on roads. In addition, whenever possible locations were included that could be readily identified and occupied during subsequent field visits in support of other quality control procedures described later. Examples of identifiable locations include manhole and other flat utility structures that have clearly indicated center points or other measurement locations. In the absence of utility structures, a PK nail was driven into asphalt or concrete and marked with paint.



 $^{^4}$ U.S. Army Corps of Engineers , Engineer Research and Development Center Topographic Engineering Center software

.

⁵ Federal Geographic Data Committee Draft Geospatial Positioning Accuracy Standards

For the Deschutes study area, 31,073 RTK (Real-time kinematic) points were collected in the study area. Figures 2.3 - 2.16 show detailed views of selected RTK locations.

Figure 2.3. Selected RTK point locations in the study area for delivery area 1; images are NAIP

orthophotos.

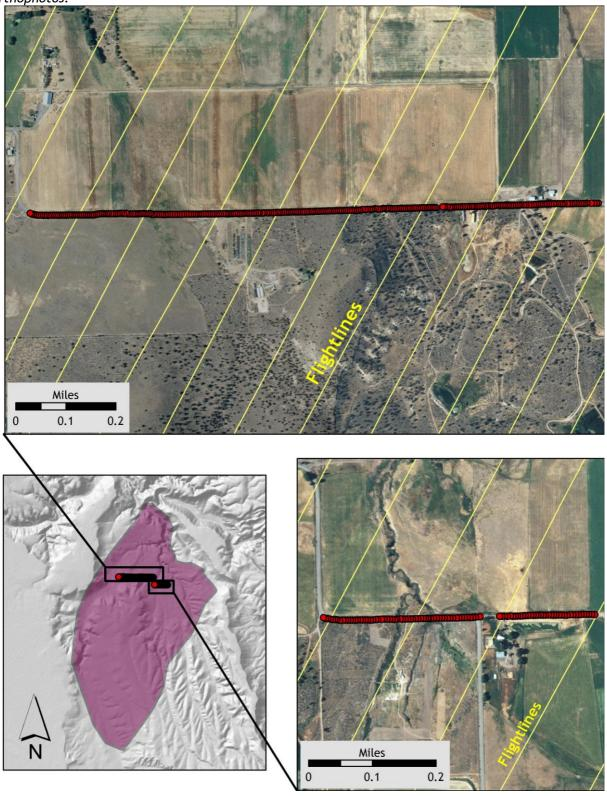
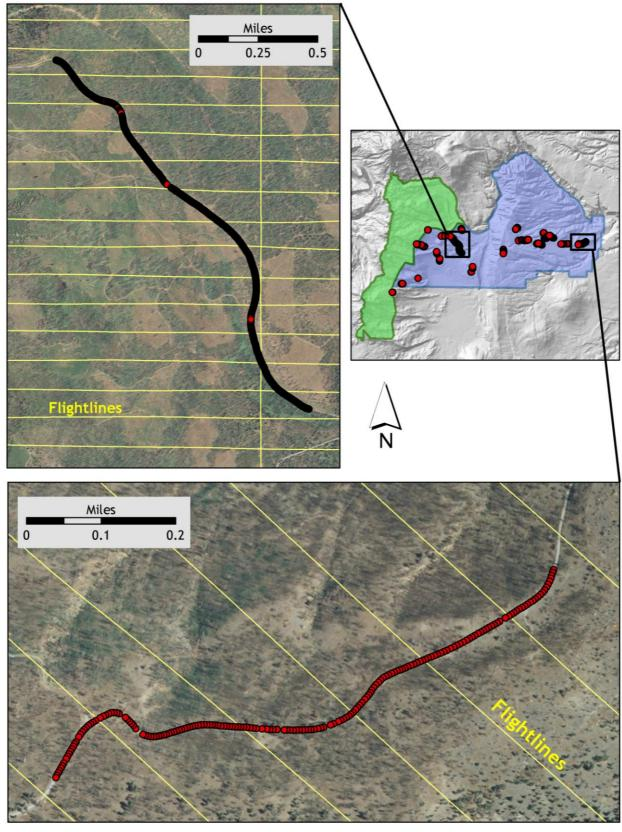


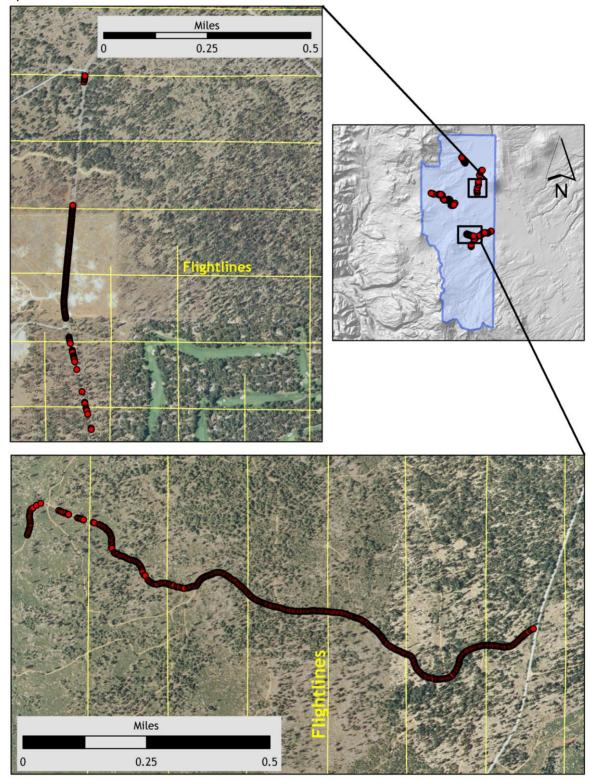
Figure 2.4. Selected RTK point locations in the study area for delivery areas 2 and 14; images are NAIP orthophotos.



Miles Miles 0.5 0.25

Figure 2.5. Selected RTK point locations in the study area for deliveries 3 and 5; images are NAIP orthophotos.

Figure 2.6. Selected RTK point locations in the study area for delivery area 4; images are NAIP orthophotos.



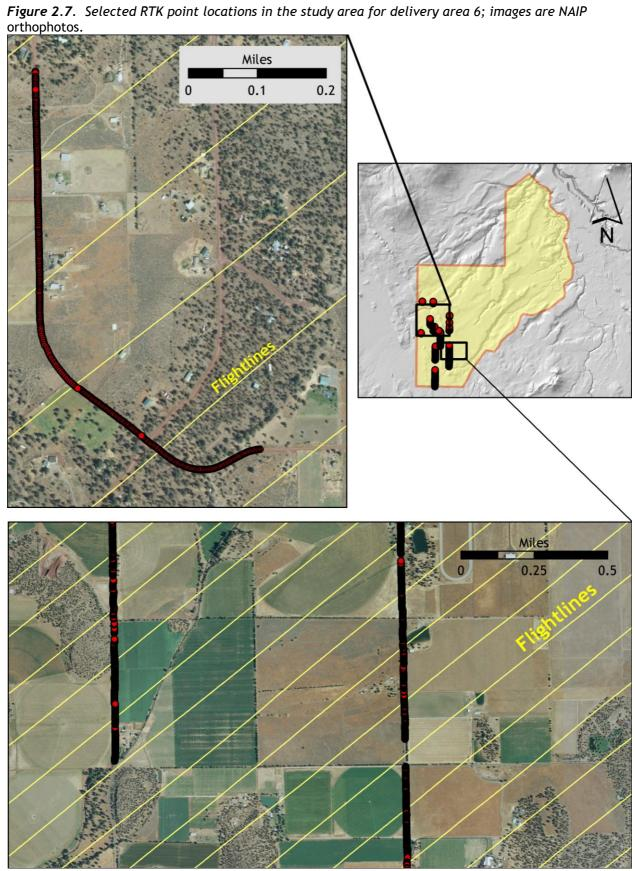


Figure 2.8. Selected RTK point locations in the study area for delivery areas 7 and 16; images are NAIP orthophotos.

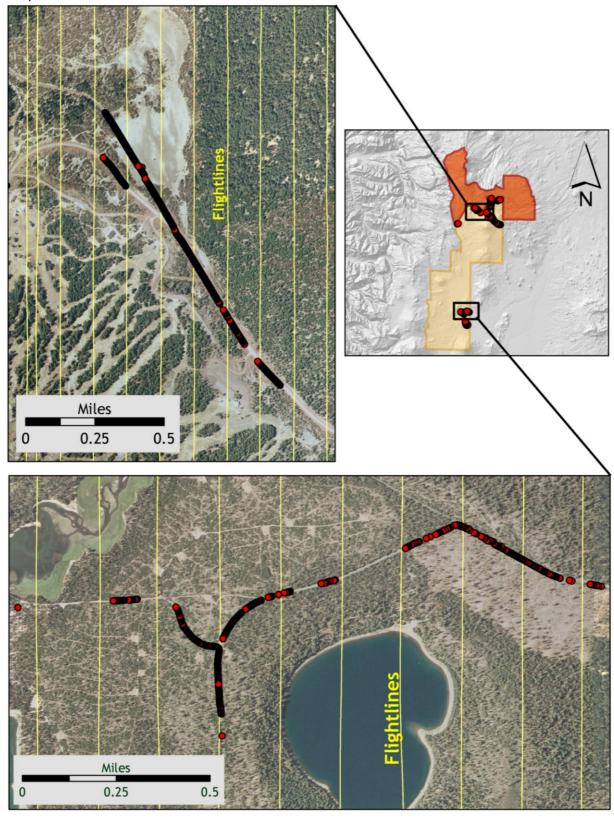
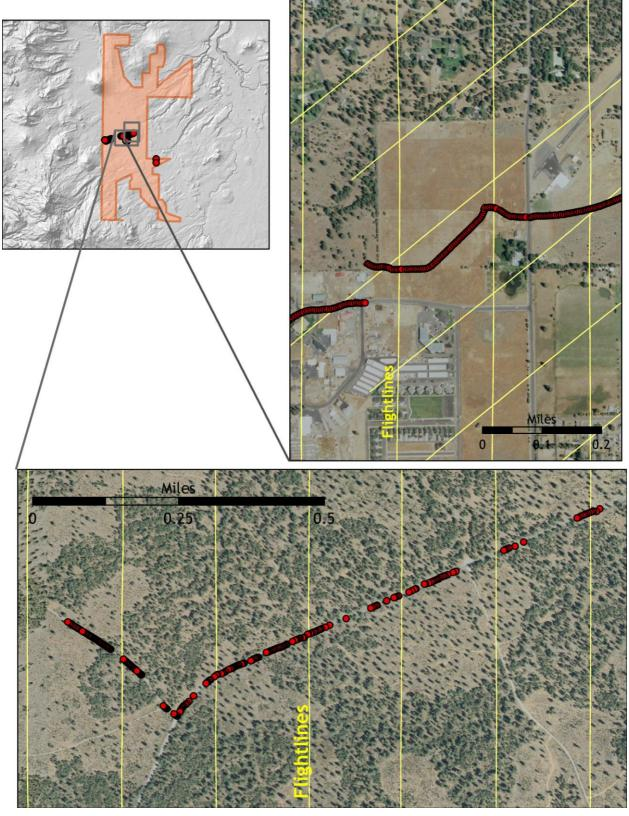


Figure 2.9. Selected RTK point locations in the study area for delivery area 8; images are NAIP orthophotos.



Miles 0.05 Miles

Figure 2.10. Selected RTK point locations in the study area for delivery area 9; images are NAIP orthophotos.

0.25 0.5 0.1 0.2

Figure 2.11. Selected RTK point locations in the study area for delivery area 10; images are NAIP orthophotos.

Figure 2.12. Selected RTK point locations in the study area for delivery area 11; images are NAIP orthophotos. Miles 0.25 0.5 Miles 0.25 0.5

Figure 2.13. Selected RTK point locations in the study area for delivery area 12; images are NAIP orthophotos.

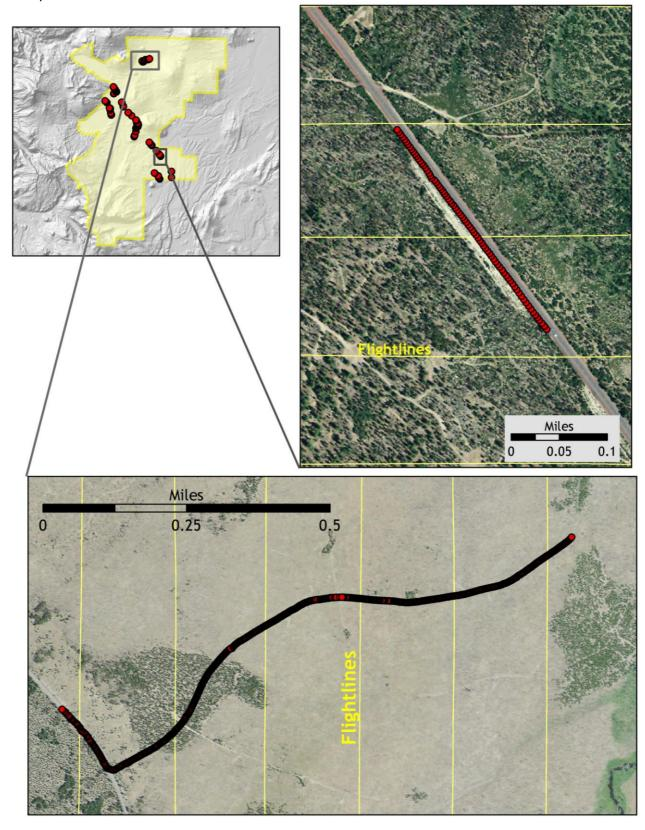


Figure 2.14. Selected RTK point locations in the study area for delivery area 13; images are NAIP orthophotos.

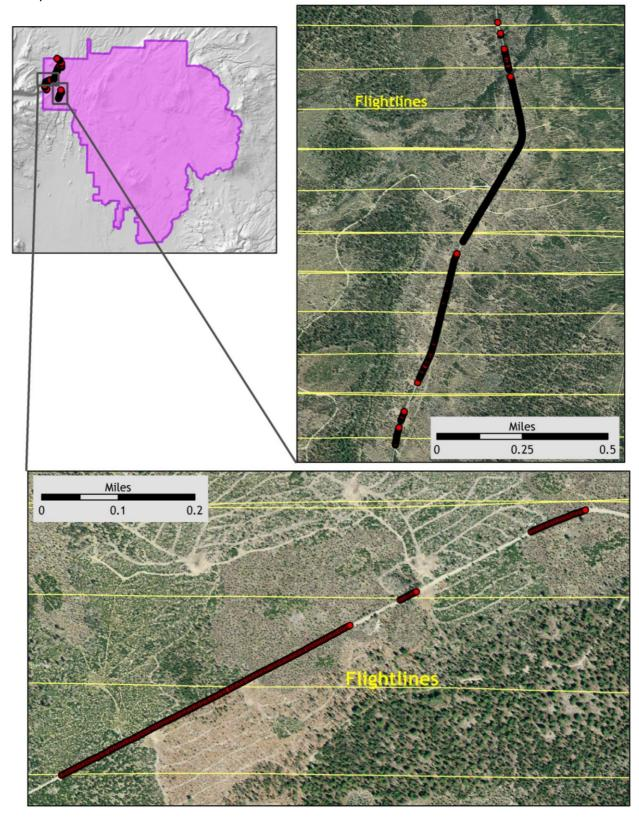


Figure 2.15. Selected RTK point locations in the study area for delivery area 15; images are NAIP orthophotos.

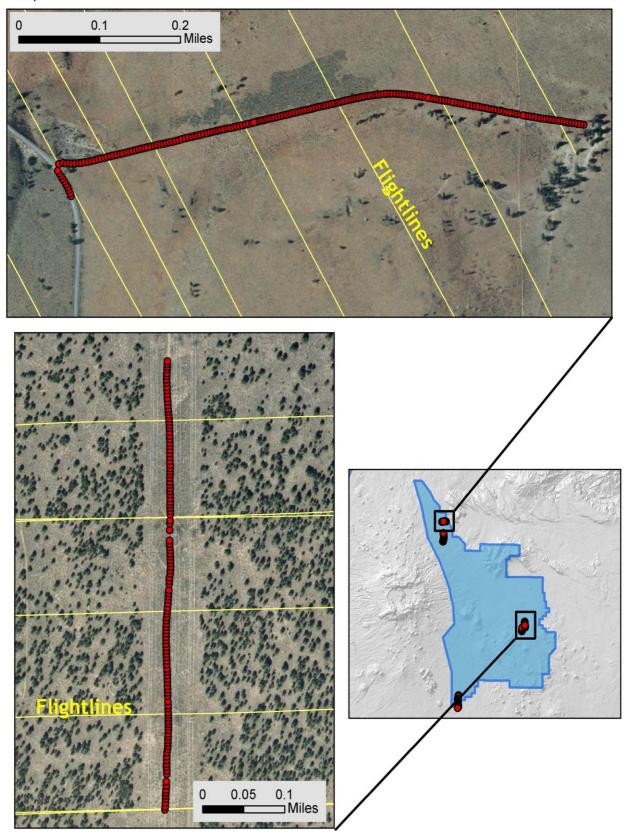
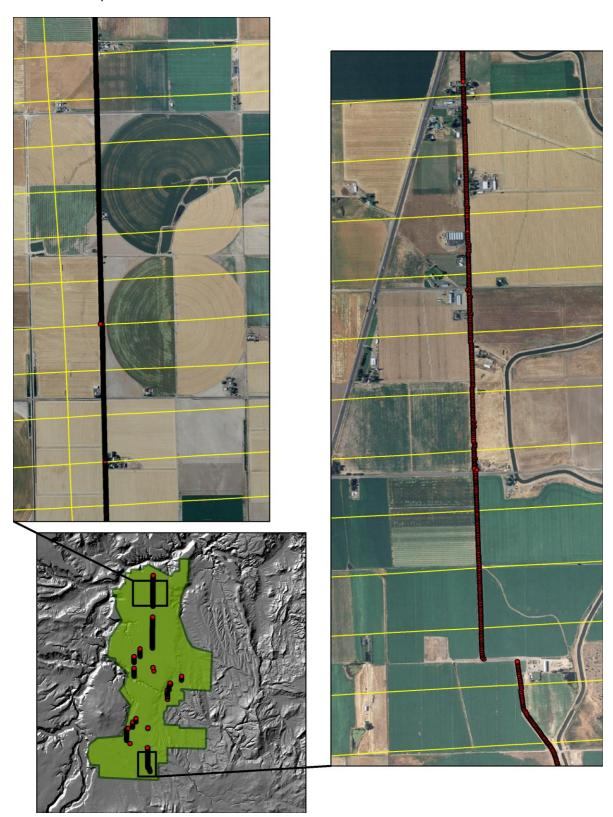


Figure 2.16. Selected RTK point locations in the study area for the current delivery, area 17; images are NAIP orthophotos.



3. Accuracy

3.1 Relative Accuracy

Relative Accuracy Calibration Results

Relative accuracy refers to the internal consistency of the data set and is measured as the divergence between points from different flightlines within an overlapping area. Divergence is most apparent when flightlines are opposing. When the LiDAR system is well calibrated, the line to line divergence is low (<10 cm). Internal consistency is affected by system attitude offsets (pitch, roll and heading), mirror flex (scale), and GPS/IMU drift.

Relative accuracy statistics are based on the comparison of 3,582 flightlines and over 95 billion points. Relative accuracy deviation statistics are reported in Figures 3.1 and 3.2.

- Project Average = 0.15 ft (0.04 m)
- Median Relative Accuracy = 0.14 ft (0.04 m)
- o 1σ Relative Accuracy = 0.16 ft (0.05 m)
- \circ 2 σ Relative Accuracy = 0.22 ft (0.07 m)

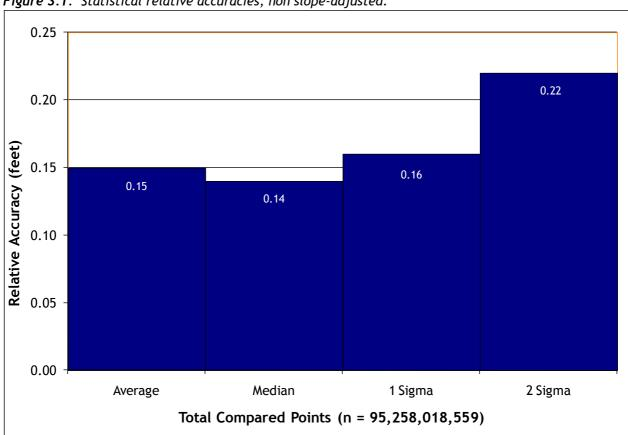


Figure 3.1. Statistical relative accuracies, non slope-adjusted.

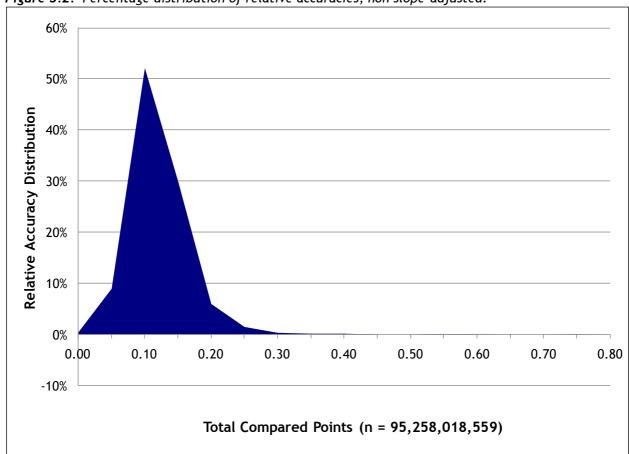


Figure 3.2. Percentage distribution of relative accuracies, non slope-adjusted.

3.2 Absolute Accuracy

Absolute accuracy compares known RTK ground survey points to the closest laser point. For the Deschutes Study Area, 31,073 RTK points were collected. Absolute accuracy is reported for the entire study and is reported in **Table 3.1** below. Histogram and absolute deviation statistics are reported in **Figures 3.3 and 3.4**.

Table 3.1. Absolute Accuracy - Deviation between laser points and RTK survey points.

| Sample Size (n): 31,073 | | | |
|--|--------------------------------|--|--|
| Root Mean Square Error (RMSE): 0.12 ft (0.04m) | | | |
| Standard Deviations | Deviations | | |
| 1 sigma (σ): 0.11 ft (0.03 m) | Minimum Δz: -0.61 ft (-0.19 m) | | |
| 2 sigma (σ): 0.24 ft (0.07 m) | Maximum Δz: 0.61 ft (0.19 m) | | |
| Average Δz: 0.09 ft (0.03 m) | | | |

Figure 3.3. Deschutes Study Area histogram statistics

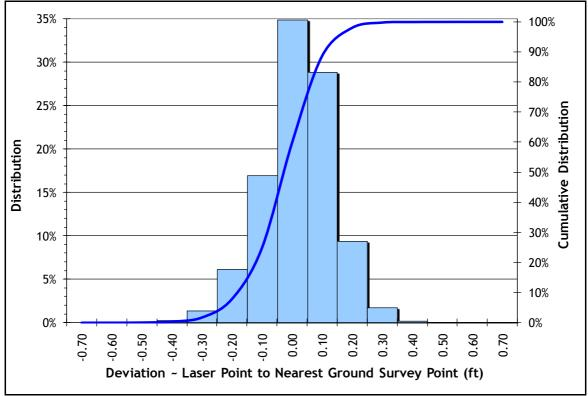
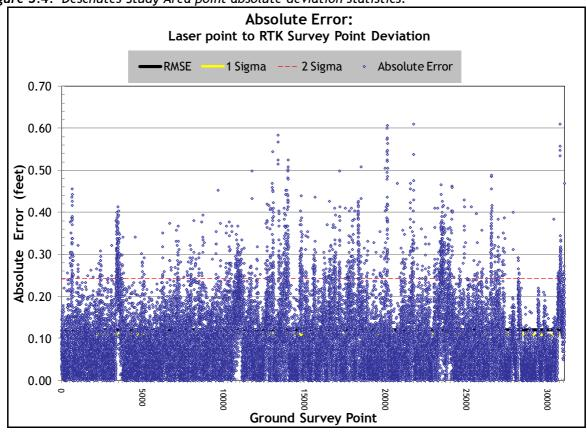


Figure 3.4. Deschutes Study Area point absolute deviation statistics.

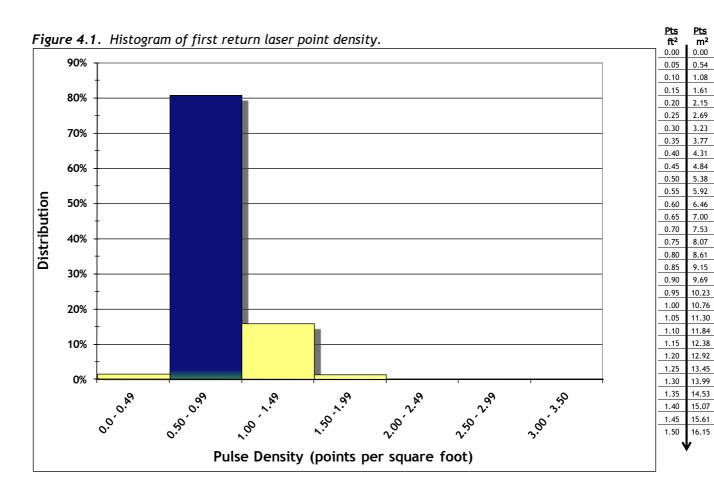


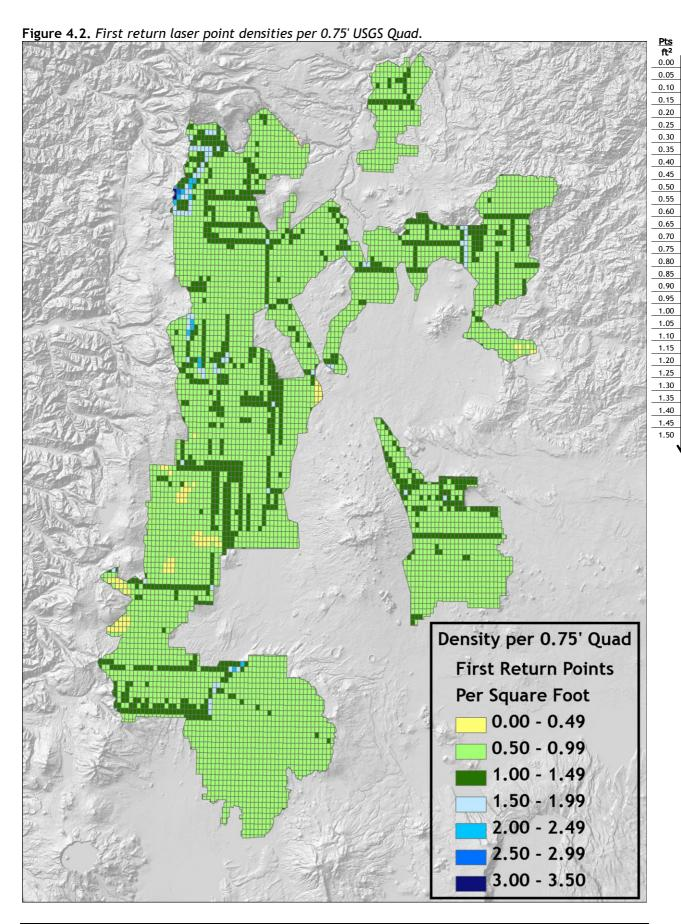
4. Data Density/Resolution

Some types of surfaces (i.e. dense vegetation or water) may return fewer pulses than the laser originally emitted. Therefore, the delivered density can be less than the native density and vary according to terrain, land cover and water bodies. Density histograms and maps (Figures 4.1 - 4.4) have been calculated based on first return laser point density and ground-classified laser point density.

Table 4.1. Average density statistics for the Deschutes Study Area.

| Average Pulse | Average Pulse | Average Ground | Average Ground |
|-----------------|----------------|-----------------|----------------|
| Density | Density | Density | Density |
| (per square ft) | (per square m) | (per square ft) | (per square m) |
| 0.87 | 9.4 | .23 | 2.5 |





2.69

3.23

4.31

7.00

7.53

8.07

8.61

9.15 9.69 10.23

11.30 11.84

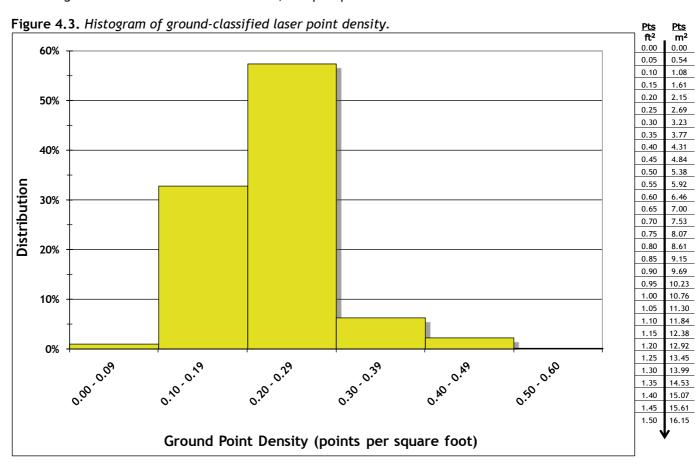
12.38

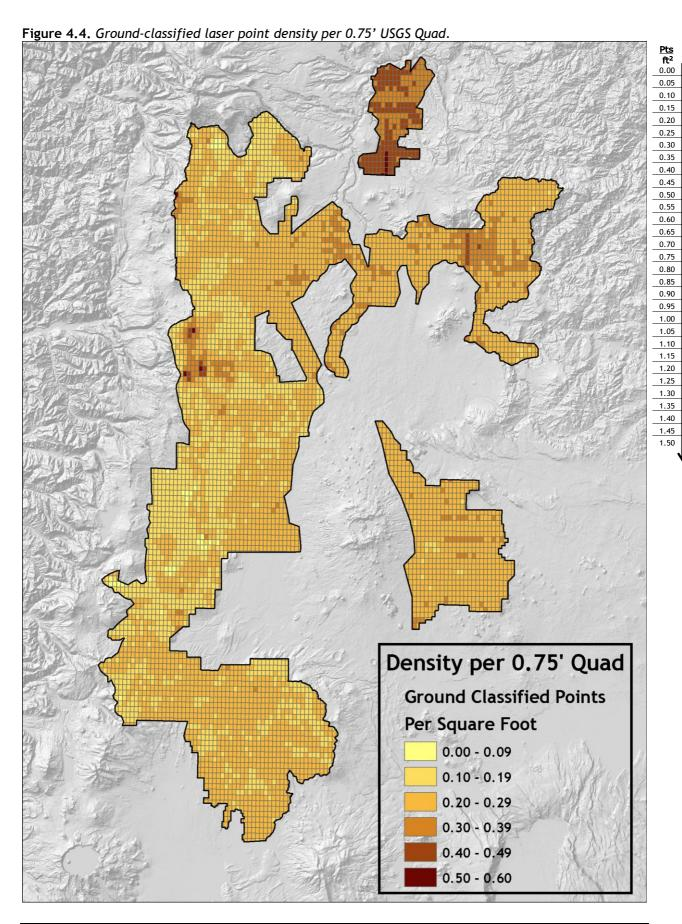
12.92

13.45 13.99 14.53 15.07

15.61

Ground classifications were derived from ground surface modeling. Classifications were performed by reseeding of the ground model where it was determined that the ground model failed, usually under dense vegetation and/or at breaks in terrain, steep slopes and at bin boundaries.





1.08

2.15

2.69

3.23

4.84

5.92

7.00 7.53 8.07

9.69

10.23

10.76

11.30

11.84 12.38 12.92 13.45 13.99 14.53 15.07

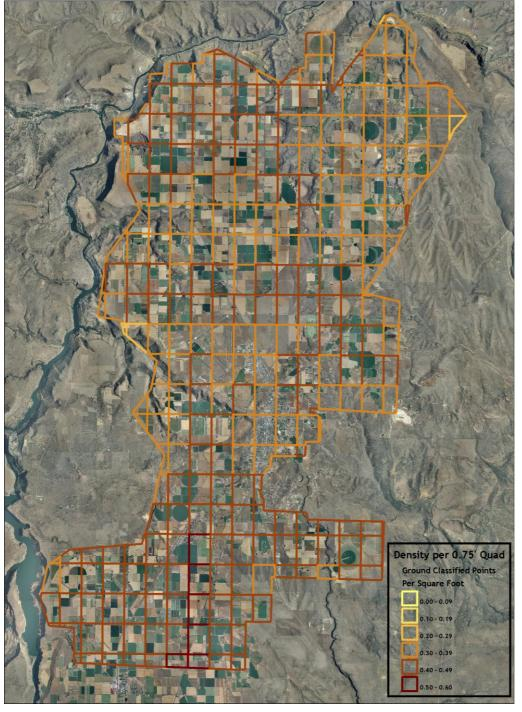
15.61

16.15

The land cover in delivery areas 1 and 17 is almost exclusively agricultural. This resulted in a high percentage of laser pulses reaching the ground and an exceptionally high ground-point density (an average of $0.40 \, p/ft^2 \, (4.32 \, p/m^2)$ per $0.75' \, quad$).

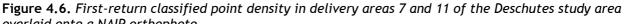
Figure 4.5. Ground-classified point density in delivery areas 1 and 17 of the Deschutes study area

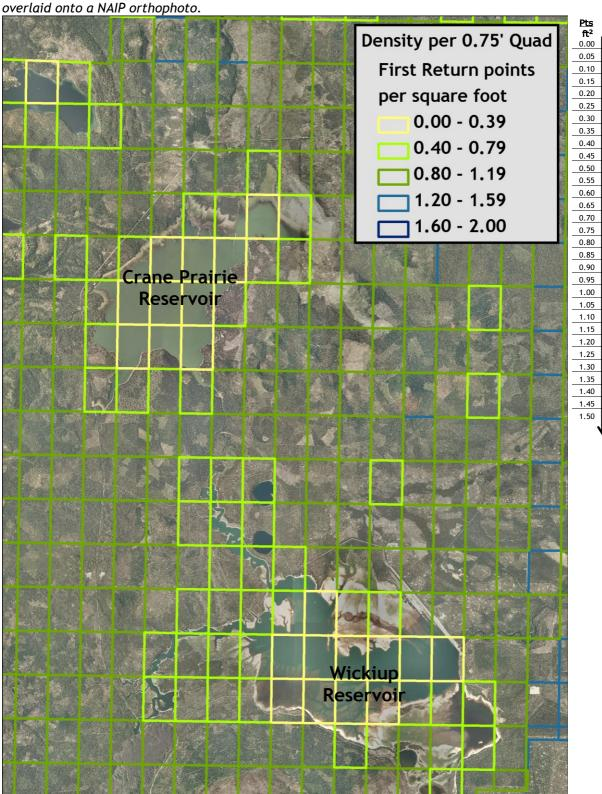
overlaid onto a NAIP orthophoto.



| Pts | Pts |
|-------------|-------|
| ft² | . m² |
| 0.00 | 0.00 |
| 0.05 | 0.54 |
| 0.10 | 1.08 |
| 0.15 | 1.61 |
| 0.20 | 2.15 |
| 0.25 | 2.69 |
| 0.30 | 3.23 |
| 0.35 | 3.77 |
| 0.40 | 4.31 |
| 0.45 | 4.84 |
| 0.50 | 5.38 |
| 0.55 | 5.92 |
| 0.60 | 6.46 |
| 0.65 | 7.00 |
| 0.70 | 7.53 |
| 0.75 | 8.07 |
| 0.80 | 8.61 |
| 0.85 | 9.15 |
| 0.90 | 9.69 |
| 0.95 | 10.23 |
| 1.00 | 10.76 |
| 1.05 | 11.30 |
| 1.10 | 11.84 |
| 1.15 | 12.38 |
| 1.20 | 12.92 |
| 1.25 | 13.45 |
| 1.30 | 13.99 |
| 1.35 | 14.53 |
| 1.40 | 15.07 |
| 1.45 | 15.61 |
| 1.50 | 16.15 |
| $lack \Psi$ | |
| • | |

Decreased first-return point density in delivery areas 7 and 11 is due to the low percentage of points returned over water. The main bodies of water causing low pulse density are Crane Prairie Reservoir and Wickiup Reservoir.





0.00

0.54

1.08

2.15

2.69

3.23

4.31

5.38

6.46

7.00

7.53

8.07

8.61

9.15

9.69

10.23

10.76

11.30

11.84 12.38

12.92

13.45

14.53

15.07 15.61

16.15

5. Certifications

Watershed Sciences provided LiDAR services for the Deschutes study area as described in this report.

I, Mathew Boyd, have reviewed the attached report for completeness and hereby state that it is a complete and accurate report of this project.

Manh Bayd

Mathew Boyd Principal Watershed Sciences, Inc.

I, Christopher W. Yotter-Brown, being first dully sworn, say that as described in the Ground Survey subsection of the Acquisition section of this report was completed by me or under my direct supervision and was completed using commonly accepted standard practices. Accuracy statistics shown in the Accuracy Section have been reviewed by me to meet National Standard for Spatial Data Accuracy.

Challe Insomi

Christopher W. Yotter-Brown, PLS Oregon & Washington Watershed Sciences, Inc Portland, OR 97204

REGISTERED PROFESSIONAL LAND SURVEYOR

6/6/2011

OREGON
JULY 13, 2004
Christopher W. Yotter - Brown

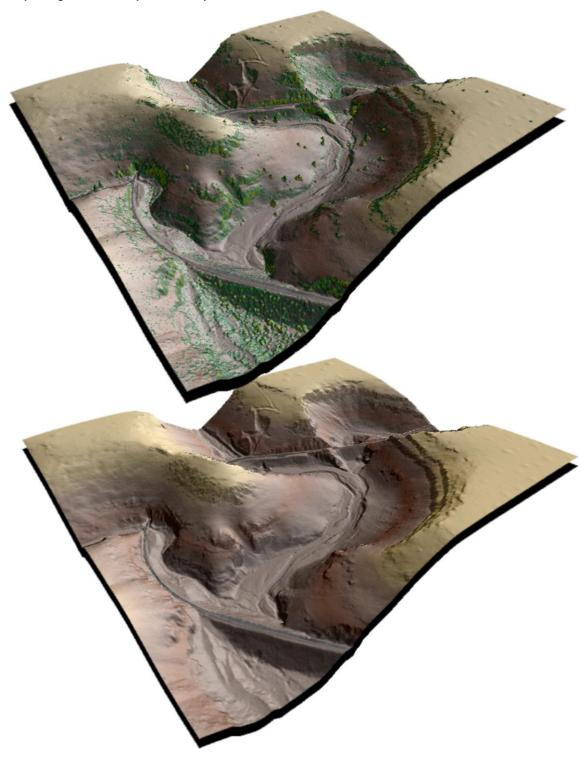
60438 LS

RENEWAL DATE: 6/30/2012

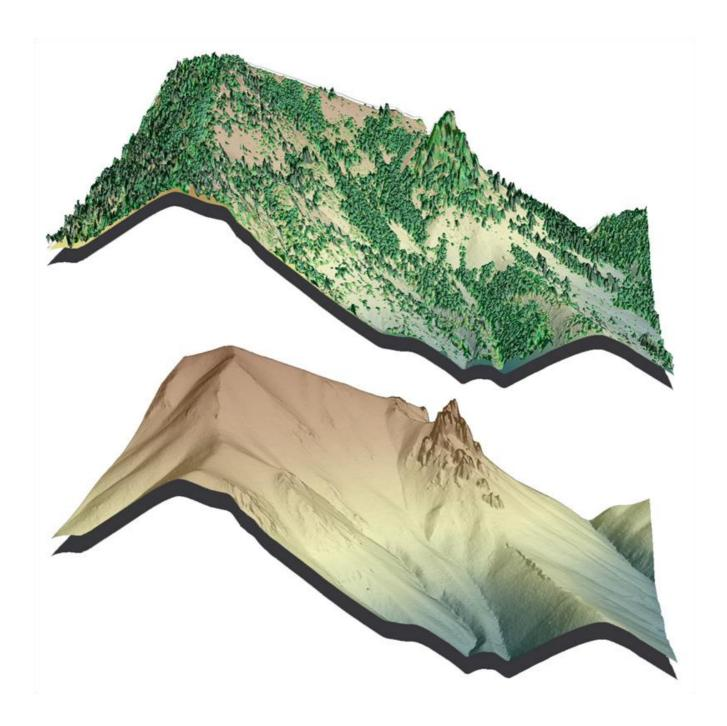
[This page intentionally left blank]

6. Selected Imagery

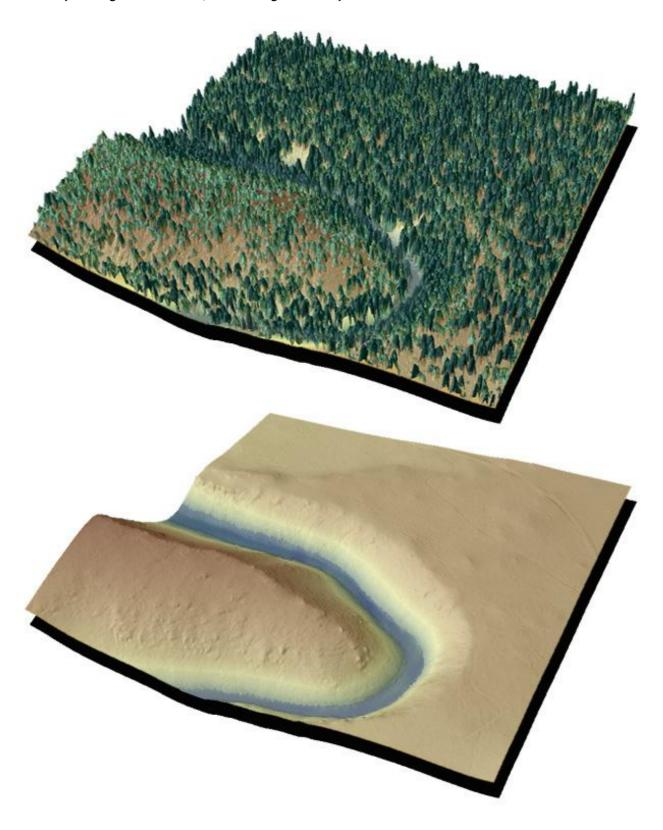
3-d oblique view of canyon lands north of Old Maid's Canyon and northeast of Madras, OR. The upper image is derived from ground-classified and highest hit LiDAR points while the lower image was created from ground-classified LiDAR points.



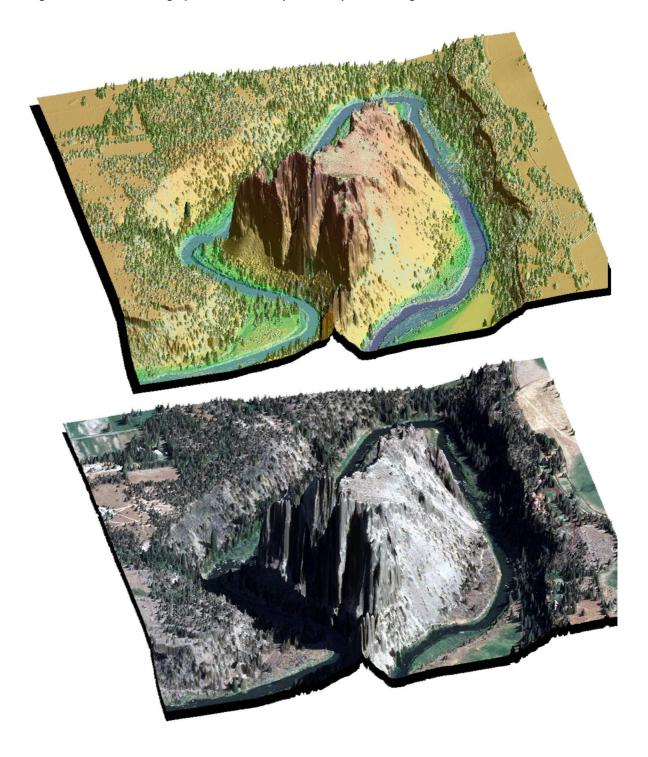
View of Gothic Rock and surrounding area in north central Oregon. Top image derived from highest hit LiDAR, lower image derived from bare earth LiDAR.



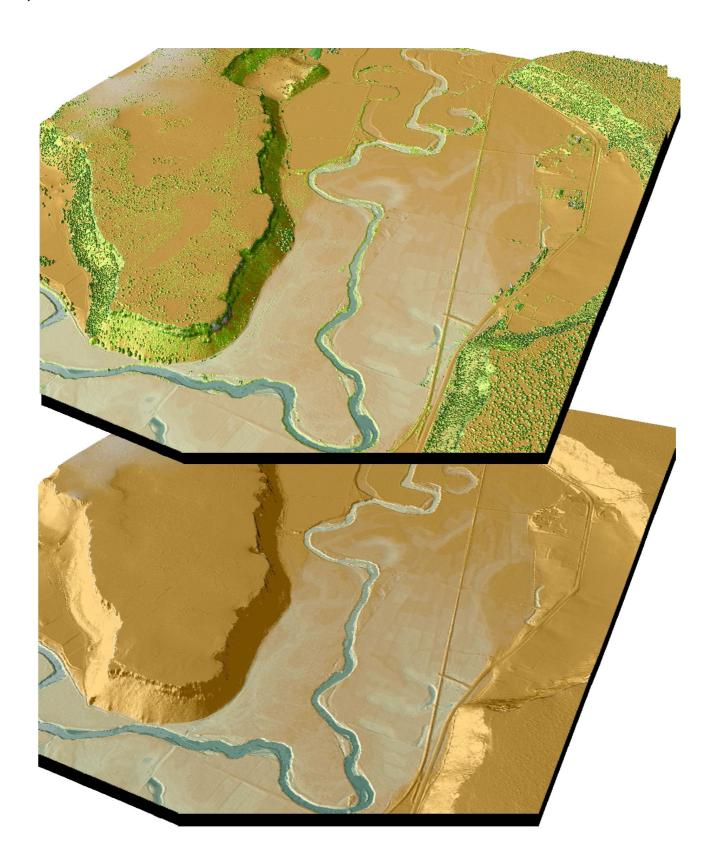
View of forested land north of Hwy 20, along the Metolius River in north central Oregon. Top image derived from highest hit LiDAR, lower image derived from bare earth LiDAR.

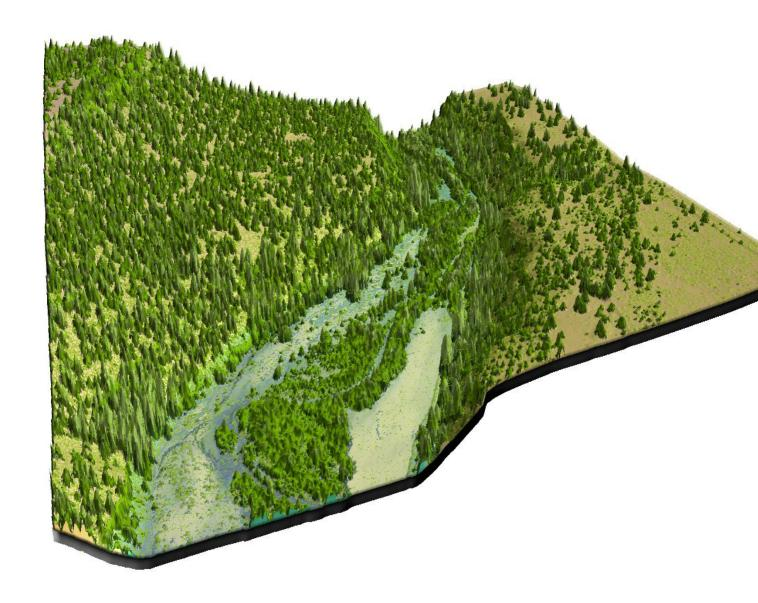


View of Smith Rock State Park and Crooked River, near Terrebonne, OR. Top image is derived from LiDAR highest hits, lower image from NAIP orthophoto draped over highest hit LiDAR.

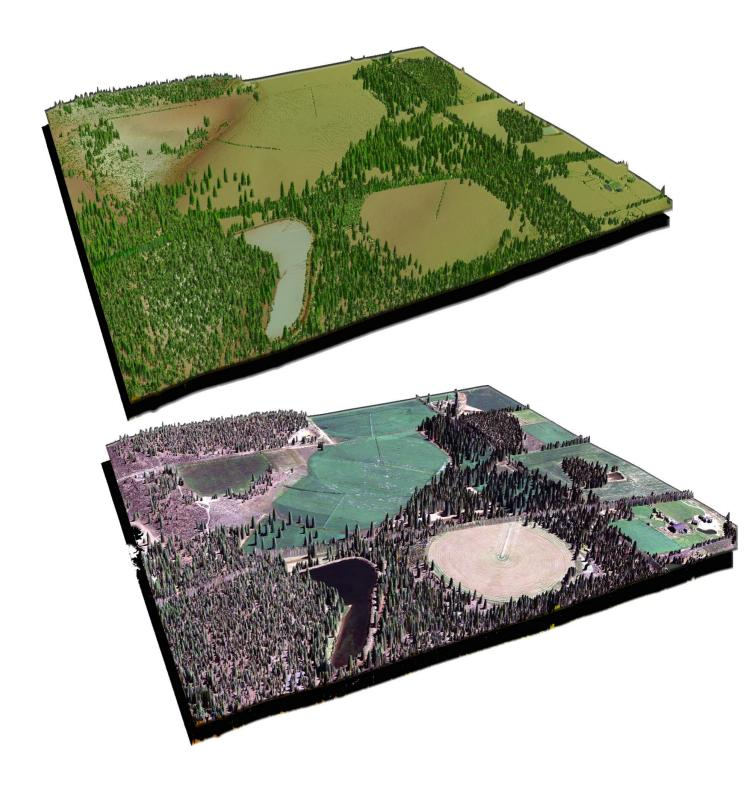


The Crooked River near Terrebonne, OR. Top image is derived from highest hit LiDAR, bottom image from bare earth LiDAR.

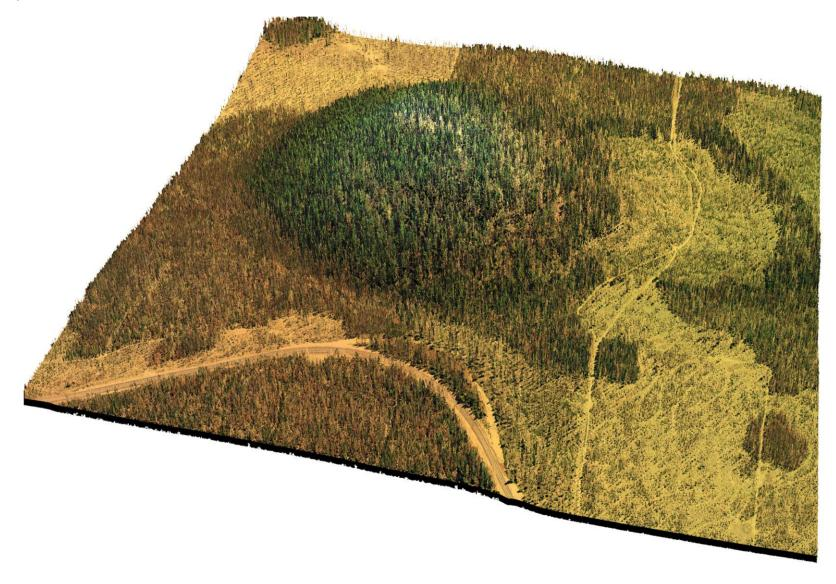




Ranch near Sisters, Oregon. Top image derived from highest hit LiDAR, bottom image created from NAIP orthophoto draped over highest hit LiDAR.



Forested land along State Highway 372, west of the city of Bend. Image created from LiDAR point cloud with RBG values extracted from NAIP orthophoto.



Mount Bachelor, west of the city of Bend. Image created from LiDAR point cloud with RBG values extracted from NAIP orthophoto.

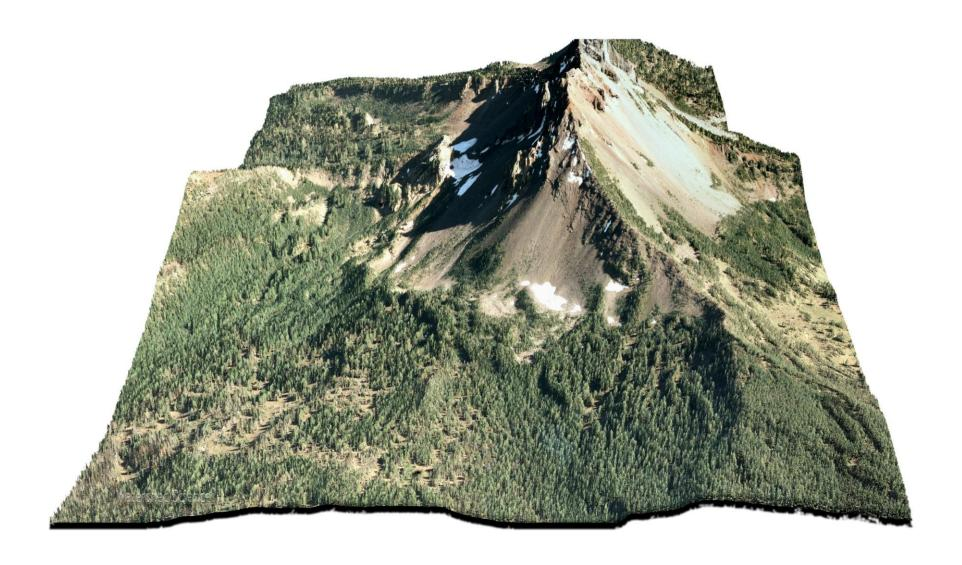


Belknap Crater, viewed from the southwest. Image created from LiDAR point cloud with RGB values extracted from NAIP orthophoto.



48

Mt. Washington viewed from the north. Image created from LiDAR point cloud with RGB values extracted from NAIP orthophoto.



The Crooked River below the Bowman Dam and Prineville Reservoir, OR. Image created from LiDAR point cloud with RGB values extracted from NAIP orthophoto.



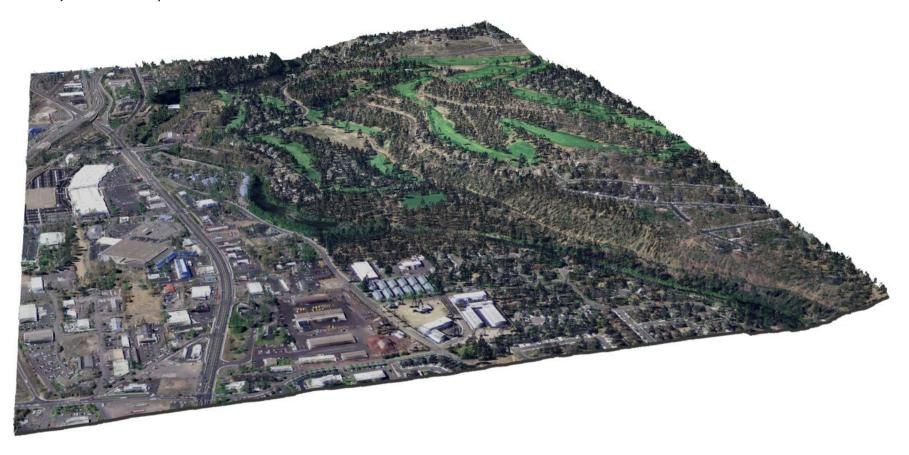
The Crooked River south of Prineville, OR. Image created from LiDAR point cloud with RGB values extracted from NAIP orthophoto.



Gopher Gulch Airstrip, south of Tumalo State Park, OR. Image created from LiDAR point cloud with RGB values extracted from NAIP orthophoto.



Riverview Park Golf Course and Highway 97 along the Deschutes River, North of Bend, OR. Image created from LiDAR point cloud with RGB values extracted from NAIP orthophoto.



Cliffs near Tumalo Falls, on Tumalo Creek. Image created with a three dimensional LiDAR point cloud with RGB values extracted from NAIP orthophotos.



Andesite volcano cone west of Sun River, Oregon. Image created with a three dimensional LiDAR point cloud with RGB values extracted from NAIP orthophotos.



Ski hill on Willamette Pass. Image created with a three dimensional LiDAR point cloud with RGB values extracted from NAIP orthophotos.

Lava Flow along Crescent Cutoff Road, OR. View is from the Northeast. Image created with a three dimensional LiDAR point cloud with RGB values extracted from NAIP orthophotos.

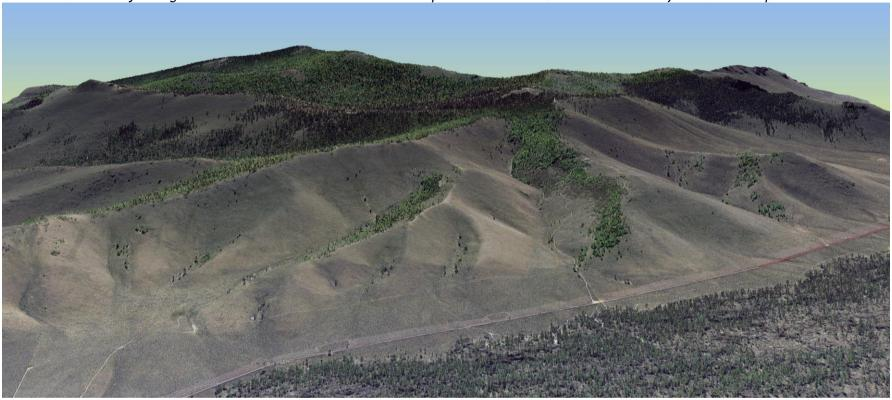


Odell Butte is a shield Volcano and the lava flow occurred 4740 years ago. It is near David Lake in Deschutes National Forest. Image created with a three dimensional LiDAR point cloud with RGB values extracted from NAIP orthophotos.



58

View from the west of Pine Mountain, Oregon. Pine Mountain is located about 30 miles southeast of Bend, Oregon and is home to the Pine Mountain Observatory. Image created with a three dimensional LiDAR point cloud with RGB values extracted from NAIP orthophotos.



View from the east of Three Finger Jack located in the Mount Jefferson Wilderness. Image created with a three dimensional LiDAR point cloud with RGB values extracted from NAIP orthophotos.

